Ceramics-Silikáty 69 (2), 361-373 (2025)
www.ceramics-silikaty.cz doi: 10.13168/cs.2025.0020

ISOLATION OF CELLULOSE NANOFIBRILS FROM *Enteromorpha prolifera* AND ITS REINFORCEMENT CAPABILITY FOR CEMENTITIOUS COMPOSITES

JIAN BAI*, **, YE YUAN**, YIMING YANG**, YANRAN LIN**, XIAOQUAN LUO**, XINYANG WANG**, #YIHONG ZHOU*, ***

*Key Laboratory of Construction and Safety of Water Engineering of the Ministry of Water Resources, China Institute of Water Resources and Hydropower Research, Beijing 100000, China
**School of Water Conservancy and Environment, University of Jinan, Jinan 250022, China
***School of Civil Engineering, Architecture and Environment, Hubei University of Technology, Wuhan 430068, China

#E-mail: zhouyihong@hbut.edu.cn

Submitted February 16, 2025, accepted March 17, 2025

Keywords: Cellulose nanofibrils, *Enteromorpha prolifera*, Microwave-assisted alkali treatment, High-intensity ultrasonication, Mechanical properties

In this study, Enteromorpha-based cellulose nanofibrils (ECNFs) were isolated from Enteromorpha prolifera, a coastal algal biomass, through a sustainable process involving microwave-assisted alkali treatment, bleaching, demineralisation, and high-intensity ultrasonication. The isolated ECNF exhibited a high aspect ratio, with an average diameter of 25.7 nm and a length of several micrometres, and demonstrated excellent thermal stability with a maximum degradation temperature of 345 °C. When incorporated into cement mortar, the ECNFs significantly enhanced the mechanical properties of the composites. At an optimal dosage of 0.05 wt. %, ECNFs improved the compressive and flexural strengths of the mortar by 12.7 % and 16.7 %, respectively, after 7 days of curing. This reinforcement effect was superior to that achieved with commercial cellulose nanofibrils (CCNFs), attributed to ECNF's larger specific surface area, higher water retention capacity, and nanoscale bridging ability, which contributed to a denser and more uniform microstructure. The findings highlight the potential of ECNFs as a sustainable and effective reinforcement material for cementitious composites, offering a sustainable approach to utilizing algal waste for high-performance construction applications.

INTRODUCTION

Phytoplankton blooms can jeopardise marine ecosystems, such as the deterioration of seawater quality, hypoxia in the water column, killing fish, and even affecting human health [1]. Currently, marine red tide has become one of the most serious problems jeopardising marine ecosystems [2]. As a typical marine alga, *Enteromorpha prolifera*, a derivative of Ulva prolifera, is widely distributed along the eastern coast of China. With global climate change and eutrophication of water bodies, more than 1,000 km of coastline are affected every year. In particular, in Qingdao, Shandong Province, the end of the coastline is inundated by seawater, posing a serious threat to the development of coastal fisheries and tourism [3].

Currently, algae landfill treatment is a method of directly burying the algal biomass in the soil. Although simple and low-cost in some respects, it is not a sustainable treatment method because of its negative environmental impacts and failure to fully utilise the resource potential of algal biomass. As one of the most abundant natural biopolymers and renewable materials, cellulose has been successfully applied in various fields due to its low cost, abundant source, and environmental friendliness [4, 5]. In addition, with the development of nanotechnology in several industries, there is a growing interest in nanomaterials [6-8]. Therefore, a considerable amount of work has been conducted on the isolation and characterisation of nanocellulose in advanced materials [9-11]. If algae can be effectively treated through a combination of chemical pre-treatments and mechanical fibrillation to isolate cellulose nanofibrils (CNFs), excess algae can be converted into a valuable resource. The application potential of algae resources is huge, and its rational utilisation not only will solve environmental problems but will also provide a new source of economic income [12].

CNF is characterised by high Young's modulus, high tensile strength, large aspect ratio, large specific surface area, small size effect and high reactivity [13-16]. In the past, CNFs were mainly produced using lignocellulosic materials from terrestrial plants, such as wood, legumes, cotton, sugarcane, straw and coffee bark [13, 17]. However, the process of isolating cellulose from wood requires lignin removal, which involves the

harsh chemical treatment of the biomass and results in the partial degradation of the cellulose. In addition, delignification is energy-intensive and the resulting cellulosic material may contain chemicals left over from the lignin removal process [18].

Algae, as a biomass resource, have become a focus of research due to their rapid growth and easy harvesting [19]. CNFs have been successfully isolated from red, brown and green macroalgae, and the cellulose content of different species of macroalgae varies considerably, ranging from 1-20 % [20]. The cellulose content also varies seasonally and is highly dependent on the biomass maturity. Different isolation methods such as chemical treatments, enzymatic treatments and physical methods have been used to isolate cellulose from algae and have been further processed on the nanoscale for use in a variety of industrial applications, demonstrating its wide range of possibilities and versatility [9, 21-23].

Fibre-reinforced cement and concrete has been shown to significantly enhance the mechanical properties and durability of materials [24]. Nanoscale cellulose, due to its high specific surface area and excellent mechanical properties, is particularly suitable for reinforcement of cementitious composites [1, 25].

This study aims to explore the isolation of *Enteromorpha*-based cellulose nanofibrils (ECNFs) and conduct a preliminary study on the mechanical properties in cement mortar to promote environmental protection and sustainable development of biomass resource utilisation. In this study, a combination of microwave-assisted alkali treatment and high-intensity ultrasonication was investigated for the isolation of ECNFs from the vast waste *Enteromorpha prolifera* growing in the coastal areas of eastern China. Microwave radiation was used as an alternative input energy source due to its ability to generate heat quickly, and the preparation process completely eliminated the dewaxing step. The traditional bleaching agent, sodium hypochlorite, has also been replaced by the more environmentally friendly low concentration of hydrogen peroxide.

The components in the isolation process were characterised by surface morphology analysis, Scanning Electron Microscopy (SEM) and Transmission Electron Microscopy (TEM), chemical functional group Fourier Transform Infrared (FT-IR) Spectrometry, crystallinity analysis X-ray diffraction (XRD), and thermal stability analysis as well as a Thermogravimetric Analysis (TGA). Then the effects of ECNFs on the mechanical properties of cementitious composites were investigated. Also, cellulose nanofibrils (CCNFs) isolated from commercial microcrystalline cellulose (MCC) were tested to compare the properties. Compared to traditional reinforcement materials, ECNFs offer a sustainable and eco-friendly alternative, leveraging the abundant and renewable nature of algal biomass while addressing the environmental challenges posed by algal blooms.

EXPERIMENTAL

Raw materials

Enteromorpha prolifera was obtained from the third beach of Qingdao, Shandong Province, eastern coastline of China (Figure 1). Commercial microcrystalline cellulose (MCC Avicel PH-101) was obtained from Sigma-Aldrich. Ordinary Portland Cement was P·O 42.5 grade cement was provided by Shanshui Group. The

Table 1. Chemical composition and physical properties of the cement.

Components	SiO_2	CaO	Al_2O_3	Fe_2O_3	MgO	SO_3	Na_2O	K_2O	Loss
Percent by mass (%)	20.33	62.42	4.78	2.98	3.27	3.1	0.26	0.72	2.14

Figure 1. *Enteromorpha prolifera* on the coastlines and beaches.

chemical composition is presented in Table 1. Tap water was used for the test and the sand was ISO standard sand. Sodium hydroxide, hydrogen peroxide, hydrochloric acid and other chemicals were laboratory grade and used without further purification.

Isolating CNF from algae

As shown in Figure 2, the individualised procedure included a microwave-assisted alkali treatment and high-intensity ultrasonication.

Washing and crushing: *Enteromorpha prolifera* was washed repeatedly with deionised water in order to remove any dirt and contaminants on the algae' surface, and dried at 60 ℃ in an oven. The dried algae were crushed using a crusher to create a reserve.

Microwave-assisted alkali treatment: For the alkali treatment, the algae powder samples (50 g) were pre-treated with 2.5 M NaOH (400mL) under microwave irradiation for 30 min using a microwave digestion system (M6, PreeKem, China) set at 360 W. The microwave heating also simultaneously induced the dewaxing of the biomass [26]. The slurry was washed with hot deionised water several times until the water reached a neutral pH.

Bleaching: The samples were further treated to remove any residual green pigments and any other colour impurities by suspending in 400 mL of 3 % H_2O_2 followed by heating of the mixture to 80 ℃ for 6 hours. After cooling to room temperature, the mixtures were filtered and rinsed with distilled water until the pH of the washing water was 7.

Demineralisation: The insoluble fraction was subsequently suspended in 200 mL of a 5 % (v/v) HCl solution. The resulting mixture was heated to the boiling point and then stirred at a constant temperature of 30 ℃ for 16 hours. After the reaction, the mixture was centrifuged at 5000 rpm for 15 min, and subsequently, the supernatant was carefully discarded. The isolated and purified cellulose was thoroughly washed with deionised water multiple times until the pH value of the washing water reached 7. The purified cellulose was then collected and subjected to a freeze - drying treatment. The samples obtained through this process were microfibrillated cellulose (MFC).

High-intensity ultrasonication: The samples were immersed in distilled water (concentration: ~ 0.5 % by mass) and left to swell for 24 hours. Subsequently, they were sonicated using a 1200W ultrasonication system (JY98-IIIDN, Ningbo Scientz Biotechnology Co., Ltd., China) at an 85 % oscillation amplitude for 1 hour while being placed in an ice/water bath. After ultrasonication, the final suspension was centrifuged multiple times and finally freeze-dried to obtain powdered CNF.

For comparative purposes, the MCC powder was dissolved in distilled water at a concentration of 0.5 % and allowed to soak for 24 hours. The subsequent steps were identical to those previously employed for the high-intensity ultrasonication. The final product obtained was commercial cellulose nanofibrils (CCNFs).

Preparation of the ECNF-mortar composites

The cement mortar was prepared according to the China SL/T 352-2020 standard and the US BS EN 196-1-2016 standard. The weighed cement and standard sand were poured into the mixer in the ratio of 1:3 and dry mixed for 10 - 20 s, then the ECNF suspensions with the different contents and the remaining water were sequentially added.

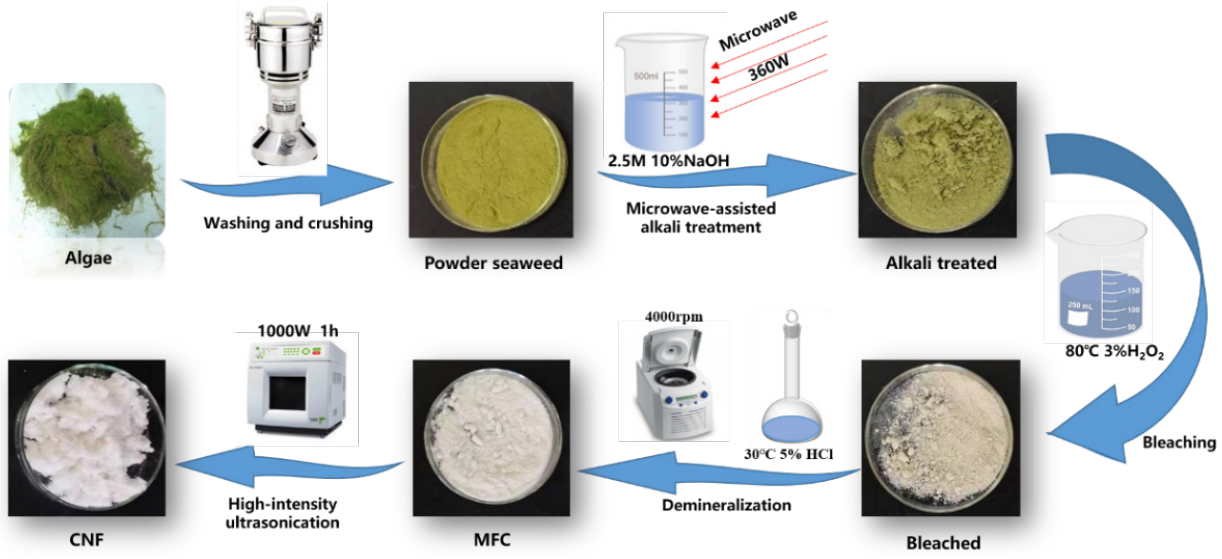

Figure 1. *Enteromorpha prolifera* on the coastlines and beaches.

The water - to - cement ratio was at 0.5, and the mixture was continuously stirred for 2 - 3 min for moulding. Then they were cured under standard curing conditions (temperature 20 ± 2 °C, relative humidity ≥ 95 %). Cementitious composites were prepared with ECNF concentrations of 0, 0.025, 0.05, 0.1, 0.3 and 0.5 wt. %. The compressive and flexural strengths were tested after 7 days of curing. The CCNF-mortar composites were prepared by the same method.

Characterisation of ECNF

Changes in the dispersion of the ECNF and CCNF suspensions were observed by visual inspection of the cellulose suspension. The specific surface area was determined by Brunauer - Emmet - Teller (BET) method. The water retention value (WRV) of the CNF samples was based on article test methods [27].

Throughout the isolation of the nanocellulose from the algae, the microscopic morphology and size of the substance after different processes were observed using SEM (Zeiss, Gemini 300). The scanning working conditions were in the secondary electron mode and the experimental parameters were a 4 nm resolution and 5 kV accelerating voltage.

The morphology of ECNF was observed by TEM (JEM 2010). A suspension of ECNF at a concentration of 5 ppm was stirred well and sonicated in an ultrasonic bath for 30 min. The well-dispersed suspension was immediately added dropwise onto a copper mesh, and then a drop of 1 % hydrogen peroxide acetate negative stain was added and left to air-dry before being observed. The accelerating voltage was 200 kV. A statistical quantification of the ECNF size was carried out by using the ImageJ software based on the $n \geq 100$ sample size for the statistical quantification of the ECNF size.

FT-IR spectra were recorded using a Tensor 27 FT-IR spectrometer from Bruker, Germany. Prior to the experiments, the samples were mixed with KBr in a mass ratio of 1/100 and pressed into transparent wafers. In each measurement, a scan resolution of 4 cm^{-1} was used based on 16 cumulative scans in the range of 4000 - 400 cm^{-1}. The crystal structure of the samples was determined and analysed using an X-ray diffractometer (Rigaku Ultima IV). The samples were scanned with Cu Kα radiation (λ = 1.5406 Å) at 40 kV and 40 mA with a scanning speed of 6°·min^{-1}, and diffractograms were recorded in the range of 10° - 80°. A mathematical model describing the relationship between the intensity and 2θ was developed on the basis of the measurement records. The crystallinity index CrI (%) of the nanocellulose was subsequently calculated according to the Segal method [28]:

$$CrI\ (\%) = \left[\frac{I_{002} - I_{am}}{I_{002}}\right] \times 100\%$$

Where I_{002} was the maximum intensity of the 002 lattice diffraction peak at 2θ = 22.4° and I_{am} was the diffraction intensity of the amorphous part at 2θ = 18°.

A thermogravimetric analyser (TA, TGA 55) was used to determine the thermal stability of the samples at a flow rate of 50 mL·min^{-1} of N_2. The experimental conditions were as follows: the heating rate was 10 °C·min^{-1}, and the temperature scanning range was from 30 °C to 800 °C. Then, N_2 was replaced with O_2 and held at 800 °C for 15 min at the same flow rate. The coke content was calculated as the weight of the sample remaining after heating in N_2 up to 800 °C, and the ash content was calculated as the mass remaining at the end of the heating procedure.

Mechanical properties of cementitious composites

A SANS electronic testing machine (MTS, CMT5504) was used for the strength testing. The flexural strength (40 mm × 40 mm × 160 mm) was subjected to a three-point bending test at a loading rate of 0.2 kN·s^{-1}, and compressive tests (40 mm × 40 mm × 40 mm) were conducted at a loading rate of 1.2 kN·s^{-1}. The mechanical properties of six mortar specimens were tested and the average strength and standard deviation were calculated.

RESULTS AND DISCUSSION

Isolation and visual examination of ECNF

Table 2 presents the yields obtained at each step of the isolating process. Based on the weight analysis, the ECNF yield was 13.7 %, which was acceptable as the cellulose content of the algae was known to be in the range of 6-35 % [29, 30].

The ECNF and CCNF suspensions with a concentration of 0.1 wt. % were prepared by ultrasonic bath for 30 min and left to stand for 30 min, as shown in Figure 3. The absence of precipitation at the bottom of the ECNF suspension bottle and the uniform dispersion indicated that a colloidal structure was obtained. In order to study the difference in the area morphology, the specific surface area was determined and the ECNFs had a larger specific surface area of 41.74 m^2·g^{-1}, while the

Table 2. Recovery yields after different isolating steps.

Isolating steps	Microwave-assisted alkalisation	Bleaching	Demineralisation	High-intensity ultrasonication
Yield (%)	50.4	36.2	20.3	13.7

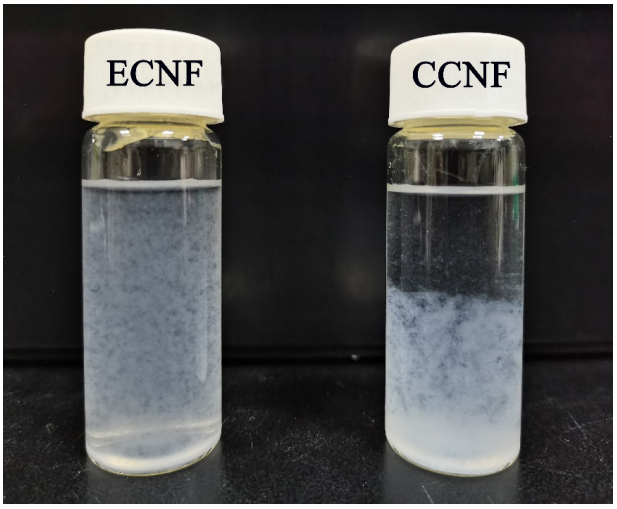

Figure 3. Suspension of ECNF and CCNF at 0.1 wt. % after 30 min of standing time.

CCNFs had a lower specific surface area of 14.81 $m^2 \cdot g^{-1}$. As well, the WRV of the ECNFs was 7.51 g/g, which was significantly higher than that of CCNF at 3.03 g/g, and we believe that it may be related to the large specific surface area of ECNFs as well as the source of nanocellulose.

Morphological analysis of ECNF

In order to explore the morphology of the cellulose at different processing stages, we characterised the SEM images at each stage, as shown in Figure 4. Figure 4. (a) and (b) show the different magnifications of the *Enteromorpha prolifera* images. In Figure 4(b) the presence of salt crystals on the surface of algae can be observed. Thus, under the crystals, a smooth fibre surface can be observed due to the presence of oils and waxes [31]. As shown in Figure 4(c), a microwave-assisted alkali treatment was performed to eliminate the protein. Figure 4(d) illustrates that the biomass structure became further loose after bleaching, which indicated that the binding forces between the microfibers in the algae were reduced. This loose structure enabled the acid to penetrate the fibres and made the reaction more effective in the next acid treatment. Figure 4(e) clearly shows that the fibre bundles were separated into the fibre structure. Figure 4(f) demonstrates that the cellulose filaments were basically isolated and intertwined into network structures after the high-intensity ultrasonication. Figure 5 exhibits the SEM images of the short-stick CCNF isolated from the MCC. In comparison, the ECNFs from *Enteromorpha prolifera* were found to be thin and long, whereas the CCNFs from the commercial MCC were short and thick.

Figure 6 displays the TEM images of the ECNFs isolated from the algae and the CCNFs isolated from the MCC. The TEM analysis exhibited that nanoscale cellulose was successfully isolated from the algae fibres. Due to the large aspect ratio, the ECNFs inevitably intertwined with each other into a network and showed typical filaments, which exhibited intermolecular hydrogen bonding and strong hydrophilic interactions between the cellulose chains [32], while the CCNFs were relatively dispersed due to their short rod shape. The length of the ECNFs was several micrometres, and the average diameter was 25.7 nm. The diameter was mainly in the range of 10 nm to 30 nm, which accounted for 71.22 % of the total, while the diameters of the ECNFs larger the 30 nm only accounted for 15.1 %, while the average diameter of the CCNFs was 63.4 nm, and the diameter was mainly distributed between 20 - 70 nm. Compared with the CCNFs, the ECNFs have a smaller diameter, larger aspect ratio and more uniform particle size distribution.

XRD analysis of the ECNFs

The crystal structure and the crystallinity index of the cellulose fractions were estimated by XRD. The XRD patterns of the untreated algae powder, MFC, ECNF, MCC and CCNF samples are shown in Figure 7. All the samples gave rise to three peaks around 2θ = 16°, 22°, and 34°, corresponding to the crystal planes (110), (002), (004), respectively, sustaining the presence of crystalline regions, these were typical peaks for the cellulose I allomorph [33-35]. The reflection at 12°, which was assigned to the cellulose II polymorph structure, was hardly visible in the sample here. This indicated that the crystal structure of cellulose was not changed during the chemical and ultrasonic treatment.

The crystallinity index (CrI %) of each sample was calculated and listed from the XRD diffractograms. According to the Segal method, the crystallinity index of CCNF was calculated to be 69.3 %, while the crystallinity index of ECNF was 63.1 %. We were surprised to find that both the ECNFs and CCNFs had a similar slight change in crystallinity index compared with the MFC and MCC, indicating that the ultrasonication process hardly changed the crystallinity and that the ultrasonication process was non-selective [36, 37]. The low crystallinity of ECNF can be explained by the samples being a mixture of cellulose and xyloglucan. The xyloglucan residue might possibly interrupt the formation of cellulose crystals leading to the low crystallinity. A significant increase in crystallinity from 9.2 % for the original algae to 57.7 % for the MFC was observed. Through the treatment, a partial removal of the xylose-glucose polysaccharide mixed with cellulose in the fractions and hemicellulose and lignin, which exist in amorphous regions [38-40]. This would explain why the MFC and ECNF had a higher crystallinity index than the *Enteromorpha prolifera*. Overall, the degree of crystallinity of the algae cellulose seems to be low. In some algae, cellulose was the major component of the cell wall and the cellulose tended to be highly crystalline while other algae were characterised

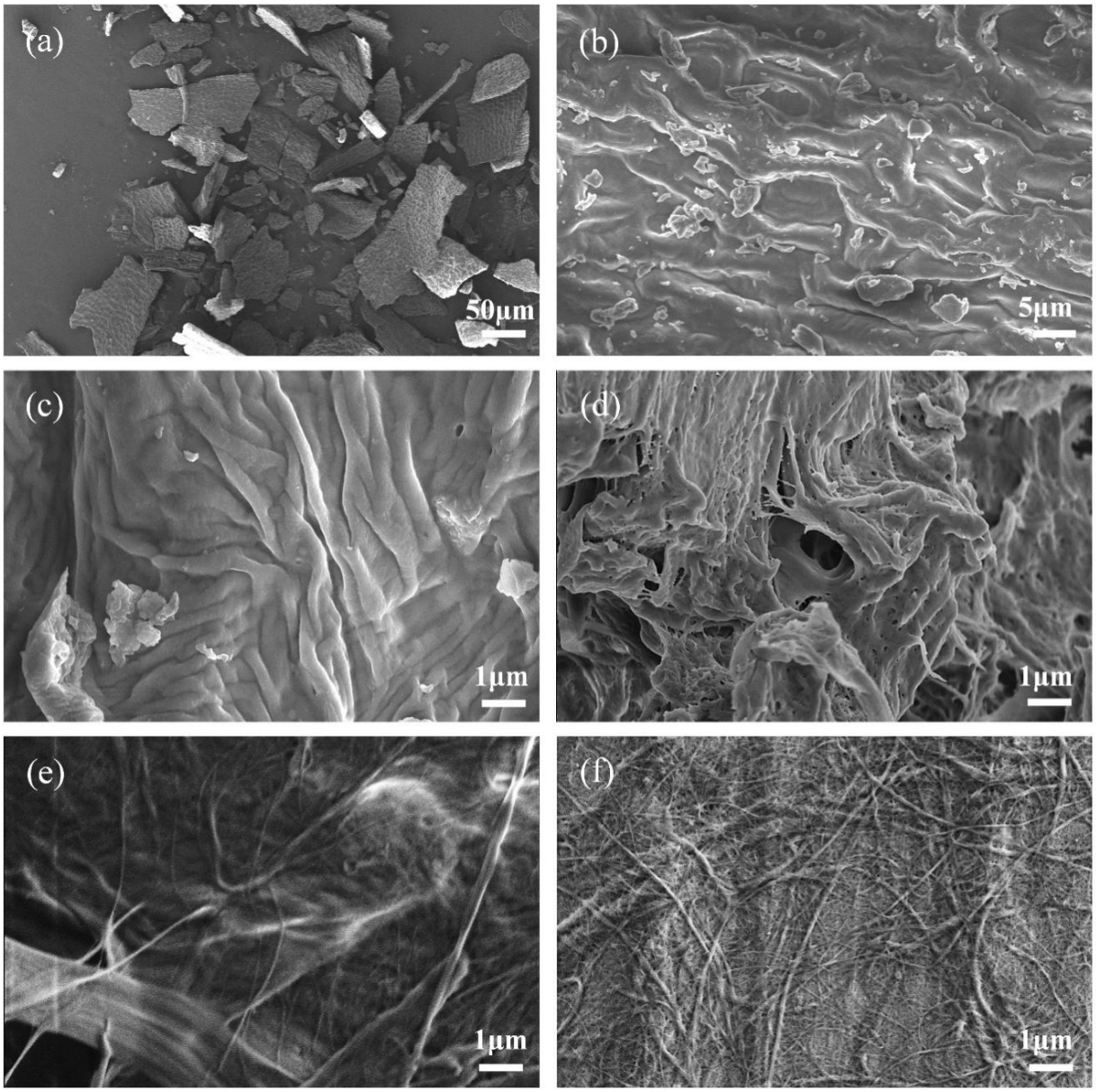

Figure 4. SEM images of (a) and (b) Enteromorpha prolifera, (c) Microwave-assisted alkali treatment, (d) Bleaching, (e) Demineralisation, (f) ECNFs.

by low contents and crystallinity of cell wall cellulose. In general, the crystallinity of ECNF depends on the source of biomass and the isolation method, with the use of strong acid treatments yielding highly crystalline cellulose and mechanical treatments yielding relatively low crystallinity [41]. In addition, the increase in the fibre crystallinity after high-intensity ultrasonication can be attributed to the removal of residual lignin and hemicellulose [42].

FT-IR analysis of the CNF

The chemical structure changes in the samples were analysed with FT-IR, and the spectra of the samples after different treatment steps are shown in Figure 8.

The FT-IR spectra of the cellulose fractions showed many characteristic peaks of polysaccharides. There is a relatively broad band in the range of 3500 - 3200 cm^{-1}, which corresponds to the stretching vibration of free O - H groups in the cellulose structure. An obvious C-H stretching vibration was also found at 2890 cm^{-1} [43, 44]. Peaks at around 1636 cm^{-1} indicated the water-absorbing O-H groups [45]. Peaks around 1540 cm^{-1} from the *Enteromorpha prolifera* samples were characteristic for lignin to be stretched C=C from aromatic hydrocarbons, and, in other samples, these attenuated peaks indicated that lignin was reduced by the microwave treatment [33]. Other articles have received similar explanations, Doh et al. [46] believed that the absorption peak between 1440 and 1557 cm^{-1} was related to the aromatic C=C

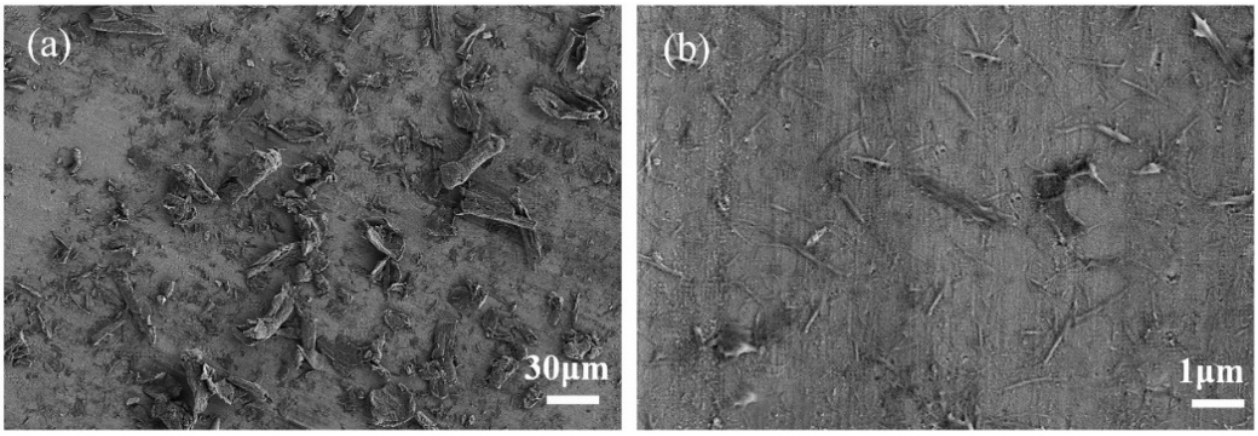

Figure 5. SEM images of the (a) MCC, (b) CCNF.

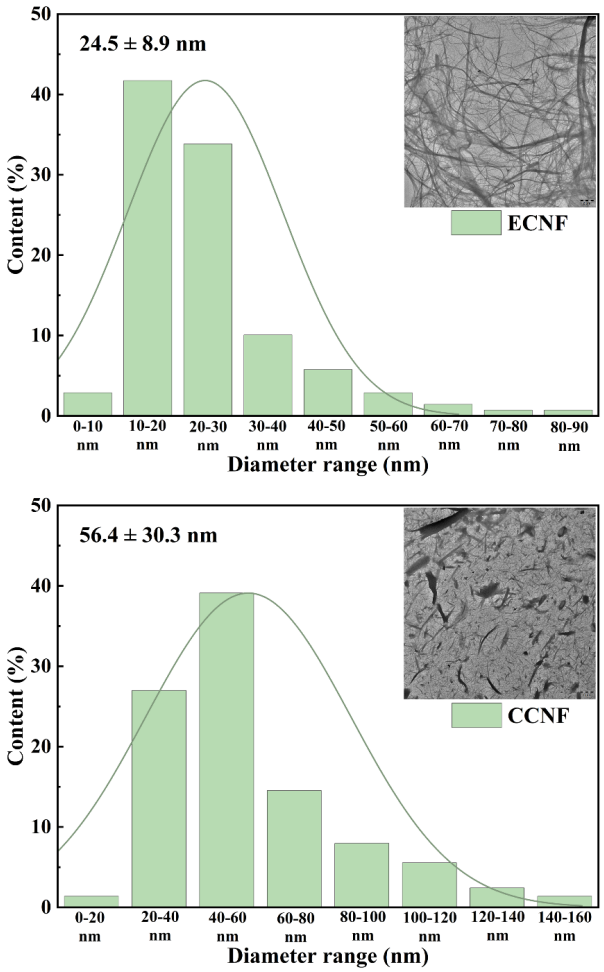

Figure 6. Diameter size distribution and TEM images of the (a) ECNF, and (b) CCNF.

in the plane symmetric stretching vibration of the aromatic ring present in lignin, and gradually decreased throughout the process. The C-H bending vibration was observed at 1372 cm^{-1} and 1315 cm^{-1}, and the in-plane bending vibrations of -CH_2 and -OCH at 1429 cm^{-1} represent cellulose groups. Similarly, the peaks near

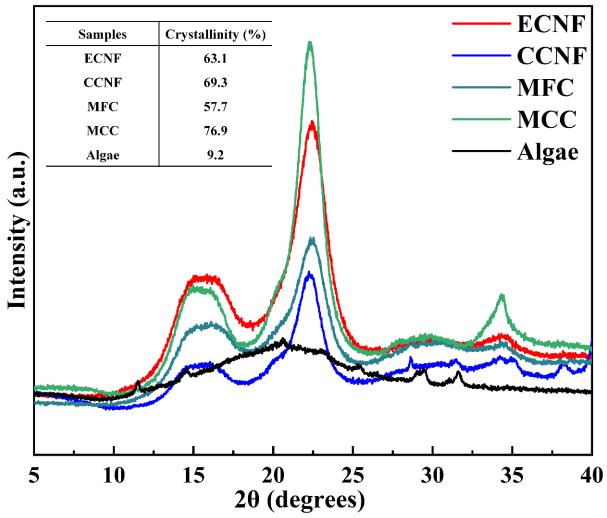

Figure 7. XRD patterns for the different types of cellulosic samples.

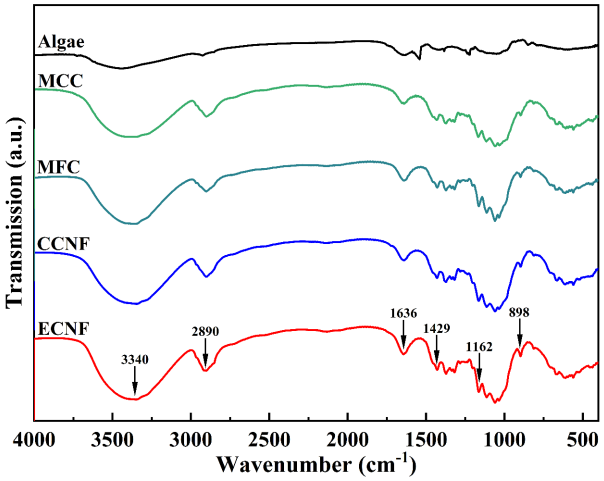

Figure 8. FT-IR spectra of the different types of cellulosic samples.

1162 cm^{-1} and 1116 cm^{-1} correspond to the asymmetric stretching vibration of the glycosidic bond C-O-C and C-OH, respectively. Moreover, the peaks near 898 cm^{-1} are due to the asymmetric stretching vibration of the β-glycosidic bond between the anhydride glucose rings in cellulose and represented the presence of amorphous region in cellulose [47]. From the untreated algae to ECNF, the increase in the intensity of the above three peaks was gradual, so we can conclude that the removal of cellulose polysaccharides exposed more cellulose content [48, 49]. The tensile vibration of the C-O-C pyranose ring skeleton in cellulose was seen at 1057 cm^{-1} [26]. The peaks at 1429, 1162, and 898cm^{-1} indicated that CNF and CCNF existed mainly in the form of cellulose I structures [46].

Compared with algae, the spectra of CNF showed no traces of strong peaks around 1220 cm^{-1} and 840 cm^{-1}, which correspond to S=O stretching and C-O-S stretching and were characteristic of the polysaccharide Ulvan. Thus, the absence of such peaks hence indicated that Ulvan was successfully removed from the cellulose fraction using the proposed fractionation protocol. Moreover, no peaks of N-H bending in proteins were observed near 1550 cm^{-1}, indicating that the cellulose samples contained only undetectable proteins with a high degree of purity [50, 51].

Thermal analysis of ECNF

The thermal stability of algae, ECNF and CCNF were further analysed using a thermogravimetric analyser, the TGA and DTG curves are shown in Figure 9. The char and ash contents are shown in Table 3, which all showed similar thermal behaviour. The weightlessness of the samples occurred at 50 - 700 °C, which was mainly divided into three stages: 50 – 150 °C, 250 – 400 °C and 500 – 800 °C. The mass of the cellulose fractions decreases by 5 % (w/w) at a temperature up to 100 °C due to the evaporation of absorbed water. It was observed in the FT-IR study that the presence of absorbing water was also detected by a peak at 1636 cm^{-1} [33, 52]. In the high temperature range, the degradation behaviour of the samples changed. All the samples had a relatively large mass loss. The algae began to degrade at 192 °C and the peak of degradation occurred at 229 °C. ECNFs were mainly weightless in the range of 251.4 - 372.3 °C, while the CCNF degradation started at a slightly higher temperature and occurred in a wide temperature range of 266.7 - 418.6 °C, which may be due to the high crystallinity which reduced the thermal degradation rate. This stage was mainly caused by the thermal degradation of cellulose itself [53]. Compared to CCNFs, ECNFs showed a slight decrease in the thermal stability, but still exhibited better thermal stability. The initial thermal decomposition (Ton) of the ECNFs was at 269 °C, and the maximum thermal degradation temperature (Td,max) was 345 °C. The CCNF initial thermal decomposition (Ton) was at 278 °C, and the maximum thermal degradation temperature (Td,max) was 360 °C. The mass loss at 500-800 °C was mainly caused by the degradation of the cellulose molecular chain. The two cellulose types exhibited the same thermal behaviour.

As shown in the graph, the amount of char residue of ECNF and CCNF were 5.7 % and 9.9 %, respectively. After the isolation process, the ash content of ECNF decreased from 24.7 (w/w) to 1.8 % (w/w), which indicated that most of the inorganic impurities

Table 3. The char and ash contents of the algae and isolated cellulose fractions.

Samples	Char % (w/w)	Ash % (w/w)
Algae	44.3	24.7
ECNF	5.7	1.8
CCNF	9.9	3.2

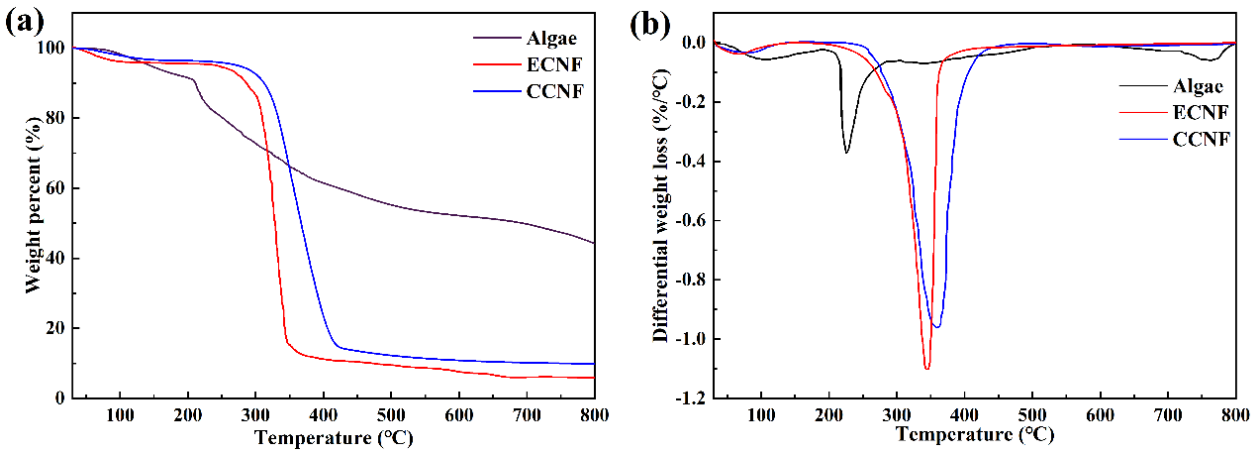

Figure 9. TGA (a) and DTG (b) curves of the algae cellulose, ECNF and CCNF.

were removed. The overall ash contents of the ECNF samples were significantly lower than that of the algae, which may be attributed to the conversion of typically water-insoluble inorganic substances such as metal oxides, carbonates and sulfates to water-soluble metal chlorides during the HCl treatment. By making these impurities water-soluble they can be removed from the cellulose since the liquid phase containing the impurities was discarded after the extraction [54]. The char and ash contents of ECNF were lower than that of CCNF, probably because more impurities were removed in the cellulose isolation process of algae, the lignin contained in the CCNF was easier to form charcoal at a high temperature, and the number of crystalline domains in the CCNF was higher. Studies have shown that the crystalline domain has inherent flame retardancy. Also, it may be that the high-intensity ultrasonication made the cellulose more dispersed, which was conducive to purification [55].

Mechanical properties of the ECNF-mortar

Table 4 illustrates the effect of the ECNFs on the compressive and flexural properties of reinforced mortar composites cured for 7 days. The results showed that the concentration of ECNFs had an important effect on the mechanical properties of the composite mortar. With the increase in the ECNF content, the compressive strength showed a tendency of increasing and then decreasing, and the strength gain reached a peak of 12.7 % when the incorporation amount of ECNF was 0.05 wt. %. Thereafter, if the doping of ECNF continues to increase above 0.1 wt. %, a decrease in strength was observed instead. The phenomenon of the mechanical properties increasing and then decreasing with the increase in the ECNF doping may be attributed to the fact that ECNF was prone to agglomeration at higher concentrations, which resulted in stress concentration points, leading to a decrease in the mechanical properties. Similarly, the trend in the flexural strength was the same as that of the compressive strength, which also showed a bell-shaped curve, and the maximum increase in flexural strength was 16.7 % when the ECNF doping was 0.05 wt. %.

In addition, we also found that the ECNF enhanced the mechanical properties of cement mortar better than CCNF, which may be due to the high aspect ratio, large specific surface area and high WRV of the ECNFs, which help to improve the denseness and uniformity of microstructure of mortar more. However, the optimum addition of ECNF to enhance the mechanical properties of mortar was lower than that of CCNF, which may be due to the fact that ECNF was more prone to agglomeration. As shown in Figure 10, we selected ECNF-reinforced composites and CCNF-reinforced composites with the largest mechanical property enhancement after 7 days of curing to observe the crack patterns of the mortar specimens. It can be seen that the presence of ECNF

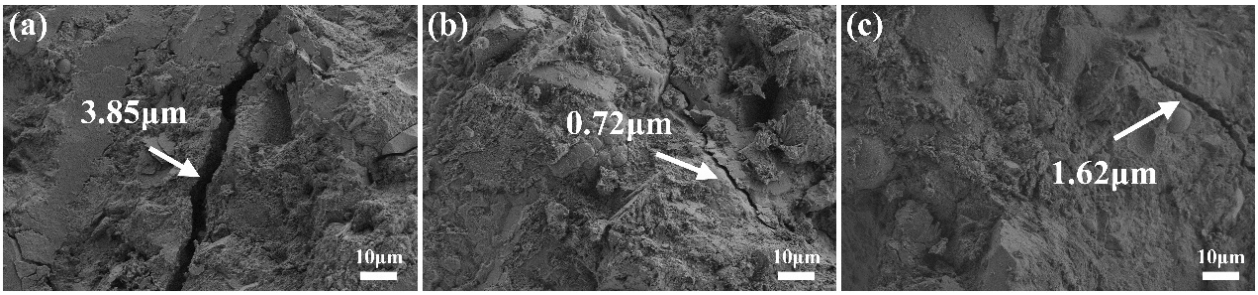

Figure 10. SEM images of the crack width on the mortar surface of the plain mortar (a), ECNF-mortar (b), and CCNF-mortar (c).

Table 4. Compressive strength and flexural strength of the different ECNF and CCNF concentrations of the mortars after 7 days.

Samples	Compressive strength (MPa)	% Increase	Flexural strength (MPa)	% Increase
Plain mortar	25.58 ± 1.34	—	5.07 ± 0.29	—
0.025 % ECNF	26.83 ± 0.66	4.9	5.58 ± 0.18	10.1
0.05 % ECNF	28.83 ± 1.45	12.7	5.91 ± 0.06	16.7
0.1 % ECNF	27.58 ± 1.82	7.8	5.60 ± 0.12	10.6
0.3 % ECNF	18.83 ± 2.20	-26.4	4.91 ± 0.31	-3.2
0.5 % ECNF	15.43 ± 0.92	-39.7	3.90 ± 0.44	-23.0
0.025 % CCNF	26.20 ± 0.88	2.4	5.36 ± 0.13	5.8
0.05 % CCNF	27.78 ± 1.26	8.6	5.48 ± 0.30	8.2
0.1 % CCNF	28.07 ± 1.41	9.7	5.67 ± 0.22	11.9
0.3 % CCNF	26.20 ± 2.19	2.4	5.50 ± 0.30	8.6
0.5 % CCNF	23.38 ± 1.09	-8.6	4.60 ± 0.25	-9.1

inhibited the extension of continuous microcracks with smaller crack spacing. The interaction between the nanomaterials and the cement matrix helped to transfer the stresses uniformly to other regions, thus reducing the stress concentration and avoiding rapid crack extension [14]. ECNFs, with their large aspect ratio, specific surface area and modulus of elasticity, can act as a bridge at the nanoscale for better cracking control [13].

DISCUSSION

Enteromorpha prolifera represents an interesting abundant and renewable biomass resource. In this study, ECNFs with high aspect ratio were successfully isolated from algae biomass by a combination of microwave-assisted alkali treatment and high-intensity ultrasonication (Figure 11), and the extraction rate and quality were within acceptable limits. Short rods of CCNF were isolated from MCC using the same high-intensity ultrasonication method. The reinforcing properties of the isolated ECNF were verified by adding it to cement mortar.

By using a microwave as an alternative energy source to alkali treatment, the traditional alkali treatment of 3 - 4h was shortened to 30 min, and the process of dewaxing is eliminated to improve the efficiency of the cellulose depolymerisation, which was a more effective and environmentally friendly isolation process [26]. The high content of chlorophyll in algae limited the fibres from over-cutting, while the microwave radiation was used as an alternative input energy source, owing to its ability to rapidly generate heat, so the biomass structure became loose [56].

The treatments used in the experiments reduced the size of the fibres from the micron to the nanometre scale, which can be explained by the cavitation effect of high-intensity ultrasonication on the formation, swelling and implosion of microbubbles in the aqueous solution [26]. The violent collapse generates micro-jets and shock waves on the surface of the pre-treated fibres, leading to an axial splitting of the eroded fibre surface. The ultrasonic shock breaks the relatively weak interfaces between the cellulose connected by the hydrogen bonds, thus separating the nanocellulose [37, 40].

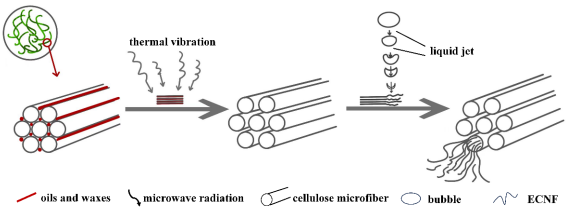

Figure 11. Schematic diagram of the ECNF isolation by combining microwave-assisted alkali and high-intensity ultrasonication.

Compared to the CCNFs, the ECNFs exhibited more remarkable reinforcement capabilities, which can be attributed to their higher specific surface area and water retention capacity. However, the propensity of ECNF to agglomerate at concentrations exceeding 0.1 wt.% is in line with findings from prior research on nanocellulose [57, 58]. Therefore, future endeavours should concentrate on refining the dispersion techniques. For instance, incorporating surfactants or making further adjustments to the ultrasonication process could alleviate agglomeration and fully exploit ECNF's reinforcing potential. Moreover, additional investigations are necessary to evaluate the long-term durability and environmental impact of ECNF-reinforced cementitious materials. The scalability of the ECNF extraction process for industrial applications also warrants in-depth exploration.

In conclusion, this study provides a sustainable and innovative approach to utilising *Enteromorpha prolifera* biomass for the production of high-performance cellulose nanofibrils. The successful application of ECNFs in cementitious composites not only addresses the environmental challenges posed by algal blooms, but also offers a promising alternative to traditional reinforcement materials, contributing to the development of eco-friendly construction technologies.

CONCLUSIONS

In this study, cellulose nanofibrils (ECNFs) were successfully isolated from *Enteromorpha prolifera* through a sustainable process combining a microwave-assisted alkali treatment and high-intensity ultrasonication. The obtained ECNFs exhibited a high aspect ratio (average diameter: 25.7 nm, length: several micrometres) and superior thermal stability (Td,max: 345°C), making it a promising candidate for reinforcing cementitious materials. The incorporation of 0.05 wt. % ECNF into the cement mortar resulted in a 12.7 % increase in compressive strength and a 16.7 % enhancement in the flexural strength compared to the plain mortar, outperforming the commercial cellulose nanofibrils (CCNFs). This improvement is attributed to the ECNF's nanoscale bridging effect, high specific surface area, and water retention capacity, which collectively promote the formation of a denser cement matrix with reduced microcrack propagation.

The utilisation of ECNFs derived from algal waste not only addresses the environmental challenges posed by coastal eutrophication, but also provides a renewable alternative to conventional reinforcement materials, significantly reducing the carbon footprint of construction composites. Future studies should focus on: (1) evaluating the long-term durability of ECNF-reinforced composites under realistic service conditions (e.g., cyclic wet-dry exposure, chloride ingress, and

freeze-thaw cycles); (2) optimising large-scale ECNF production processes to ensure the economic feasibility; and (3) exploring the synergistic effects of ECNF with other bio-based additives (e.g., biopolymers or carbon-neutral aggregates) to develop fully sustainable cementitious systems.

Acknowledgements

The authors gratefully acknowledge the financial support of the Open Research Fund of Key Laboratory of Construction and Safety of Water Engineering of the Ministry of Water Resources, China Institute of Water Resources and Hydropower Research, Grant No. 202210, and the Open Research Fund of Hubei Provincial Key Laboratory of Construction and Management in Hydropower Engineering, China Three Gorges University, Grant No. 2023KSD17. All opinions, findings, and conclusions or recommendations expressed in this material are those of the authors and do not necessarily reflect the views of the sponsoring agencies.

REFERENCES

1. Liu K., Xu Y., Wen Z., Zhang W., et al. (2023): Preparation of cellulose nanofibrils and their effects on the rheological properties and compressive strength of oil-well cement paste. *Construction and Building Materials, 394*, 132313. doi: 10.1016/j.conbuildmat.2023.132313
2. Dai Y., Yang S., Zhao D., Hu C., et al. (2023): Coastal phytoplankton blooms expand and intensify in the 21st century. *Nature, 615*(7951), 280-284. doi: 10.1038/s41586-023-05760-y
3. Zhang Q. C., Yu R. C., Chen Z. F., Qiu L. M., et al. (2018): Genetic evidence in tracking the origin of Ulva prolifera blooms in the Yellow Sea, China. *Harmful Algae, 78*, 86-94. doi: 10.1016/j.hal.2018.08.002
4. Trache D., Hussin M. H., Chuin C. T. H., Sabar S., et al. (2016): Microcrystalline cellulose: Isolation, doi: characterization and bio-composites application—A review. *International Journal of Biological Macromolecules, 93*, 789-804. doi: 10.1016/j.ijbiomac.2016.09.056
5. Patel A. K., Vadrale A. P., Singhania R. R., Michaud P., et al.. (2023): Algal polysaccharides: current status and future prospects. *Phytochemistry Reviews, 22*(4), 1167-1196. doi: 10.1007/s11101-021-09799-5
6. Szafraniec M., Grabias-Blicharz E., Barnat-Hunek D., Landis E. N. (2022): A critical review on modification methods of cement composites with nanocellulose and reaction conditions during nanocellulose production. *Materials, 15*(21), 7706. doi: 10.3390/ma15217706
7. Doh H., Lee M. H., Whiteside W. S. (2020): Physicochemical characteristics of cellulose nanocrystals isolated from seaweed biomass. *Food Hydrocolloids, 102*, 105542. doi: 10.1016/j.foodhyd.2019.105542
8. Zhao Q., Liang X., You Y., Wang Y., Du X., Liu B., Hu W. (2019): Proton conductivity improvement effect of cellulose on SPEEKK Based PEM. *Chemical Research in Chinese Universities, 35*(5), 916-923. doi: 10.1007/s40242-019-9065-x
9. Machado B., Costa S. M., Costa I., Fangueiro R., Ferreira D. P. (2024): The potential of algae as a source of cellulose and its derivatives for biomedical applications. *Cellulose, 31*(6), 3353-3376. doi: 10.1007/s10570-024-05816-w
10. García-Guzmán L., Arzate-Vázquez I., Velazquez G., Díaz-Bandera D., et al. (2024): Isolation and characterization of starch, cellulose, and their nanostructures obtained from commelina coelestis willd root. *Journal of Polymers and the Environment, 32*(9), 4550-4566. doi: 10.1007/s10924-024-03210-y
11. Yang S., Ai F., Li Z., Zhao G., Bi Y. (2022): N-doped carbon nanofibers encapsulating CoO@ Co9S8 nanoparticles: preparation from S-Rich Co32 coordination cluster precursors by electrospinning and application for superior Li-ion storage. *Chemical Research in Chinese Universities, 38*(2), 603-608. doi: 10.1007/s40242-021-1157-8
12. Ren C. G., Liu Z. Y., Zhong Z. H., Wang X. L., Qin S. (2022): Integrated biotechnology to mitigate green tides. *Environmental Pollution, 309,* 119764. doi: 10.1016/j.envpol.2022.119764
13. Santos R. F., Ribeiro J. C. L., De Carvalho J. M. F., Magalhães W. L. E., et al. (2021): Nanofibrillated cellulose and its applications in cement-based composites: A review. *Construction and Building Materials, 288*, 123122. doi: 10.1016/j.conbuildmat.2021.123122
14. Akhlaghi M. A., Bagherpour R., Kalhori H. (2020): Application of bacterial nanocellulose fibers as reinforcement in cement composites. *Construction and Building Materials, 241*, 118061. doi: 10.1016/j.conbuildmat.2020.118061
15. Chu Y., Sun Y., Wu W., Xiao H. (2020): Dispersion properties of nanocellulose: a review. *Carbohydrate Polymers, 250*, 116892. doi: 10.1016/j.carbpol.2020.116892
16. Fatima W., Tarique M., Li M., Chen M., et al. (2021): Reactive Dyeing of Electrospun Cellulose Nanofibers by Pad-steam Method. *Chemical Research in Chinese Universities, 37*(3), 535-540. doi: 10.1007/s40242-021-1107-5
17. Ewnetu Sahlie M., Zeleke T. S., Aklog Yihun F. (2022): Water Hyacinth: A sustainable cellulose source for cellulose nanofiber production and application as recycled paper reinforcement. *Journal of Polymer Research, 29*(6), 230. doi: 10.1007/s10965-022-03089-0
18. Arvidsson R., Nguyen D., Svanström M. (2015): Life cycle assessment of cellulose nanofibrils production by mechanical treatment and two different pretreatment processes. *Environmental Science & Technology, 49*(11), 6881-6890. doi: 10.1021/acs.est.5b00888
19. Zanchetta E., Damergi E., Patel B., Borgmeyer T., Pick H., Pulgarin A., Ludwig C. (2021): Algal cellulose, production and potential use in plastics: Challenges and opportunities. *Algal Research, 56*, 102288. doi: 10.1016/j.algal.2021.102288
20. Wahlström N., Nylander F., Malmhäll-Bah E., Sjövold K., Edlund U., Westman G., Albers E. (2020): Composition and structure of cell wall ulvans recovered from Ulva spp. along the Swedish west coast. *Carbohydrate Polymers, 233*, 115852. doi: 10.1016/j.carbpol.2020.115852
21. Saedi S., Kim J. T., Shokri M., Kim J. H., Shin G. H. (2023): Green seaweed (Ulva ohnoi) as a new eco-friendly source for preparing transparent and functional regenerated cellulose composite films. *Cellulose, 30*(5), 3041-3059. doi: 10.1007/s10570-023-05055-5
22. Vasques J. C., Mathias S. L., Alves L. R., Net, W. A. R., de Almeida Lucas A., de Menezes A. J. (2024): Cellulose

nanocrystals from tucum fibers cultivated in Amazon Forest: extraction and characterization. *Journal of Polymer Research, 31*(11), 330. doi: 10.1007/s10965-024-04183-1

23. Yang X., We, Y., Chu X., Zhao Q., et al. (2019): Carboxyl-functionalized nanocellulose reinforced nanocomposite proton exchange membrane. *Chemical Research in Chinese Universities, 35*(4), 735-741. doi: 10.1007/s40242-019-8330-3
24. Barnat-Hunek D., Szymańska-Chargot M., Jarosz-Hadam M., Łagód G. (2019): Effect of cellulose nanofibrils and nanocrystals on physical properties of concrete. *Construction and Building Materials, 223*, 1-11. doi: 10.1016/j.conbuildmat.2019.06.145
25. Sun B., Chao D., Wang C. (2022): Piezoelectric nanogenerator based on electrospun cellulose acetate/nanocellulose crystal composite membranes for energy harvesting application. *Chemical Research in Chinese Universities, 38*(4), 1005-1011. doi: 10.1007/s40242-021-1252-x
26. Singh S., Gaikwad K. K., Park S. I., Lee Y. S. (2017): Microwave-assisted step reduced extraction of seaweed (Gelidiella aceroso) cellulose nanocrystals. *International Journal of Biological Macromolecules, 99*, 506-510. doi: 10.1016/j.ijbiomac.2017.03.004
27. Onyianta A. J., O'Rourke D., Sun D., Popescu C. M., Dorris M. (2020): High aspect ratio cellulose nanofibrils from macroalgae Laminaria hyperborea cellulose extract via a zero-waste low energy process. *Cellulose, 27*, 7997-8010. doi: 10.1007/s10570-020-03223-5
28. Ardanuy Raso M., Claramunt Blanes J., Arévalo Peces R., Parés Sabatés F., Aracri E., Vidal Lluciá T. (2012): Nanofibrillated cellulose (NFC) as a potential reinforcement for high performance cement mortar composites. *BioResources, 7*(3), 3883-3894.
29. Jmel M. A., Messaoud G. B., Marzouki M. N., Mathlouthi M., Smaali I. (2016): Physico-chemical characterization and enzymatic functionalization of Enteromorpha sp. cellulose. *Carbohydrate Polymers, 135*, 274-279. doi: 10.1016/j.carbpol.2015.08.048
30. Thygesen A., Fernando D., Ståhl K., Daniel G., Mensah M., Meyer A. S. (2021): Cell wall configuration and ultrastructure of cellulose crystals in green seaweeds. *Cellulose, 28,* 2763-2778. doi: 10.1007/s10570-021-03698-w
31. Paniz O. G., Pereira C. M., Pacheco B. S., Wolke S. I., et al. (2020): Cellulosic material obtained from Antarctic algae biomass. *Cellulose, 27*, 113-126. doi: 10.1007/s10570-019-02794-2
32. Ono Y., Takeuchi M., Zhou Y., Isogai A. (2021): TEMPO/NaBr/NaClO and NaBr/NaClO oxidations of cotton linters and ramie cellulose samples. *Cellulose, 28*(10), 6035-6049. doi: 10.1007/s10570-021-03944-1
33. Chen Y. W., Lee H. V., Juan J. C., Phang S. M. (2016): Production of new cellulose nanomaterial from red algae marine biomass Gelidium elegans. *Carbohydrate Polymers, 151*, 1210-1219. doi: 10.1016/j.carbpol.2016.06.083
34. Liu Z., Li X., Xie W., Deng H. (2017): Extraction, isolation and characterization of nanocrystalline cellulose from industrial kelp (Laminaria japonica) waste. *Carbohydrate Polymers, 173,* 353-359. doi: 10.1016/j.carbpol.2017.05.079
35. Sung S. H., Chang Y., Han J. (2017): Development of polylactic acid nanocomposite films reinforced with cellulose nanocrystals derived from coffee silverskin. *Carbohydrate Polymers, 169*, 495-503. doi: 10.1016/j.carbpol.2017.04.037
36. Low Z. L., Low D. Y. S., Tang S. Y., Manickam S., Tan K. W., Ban Z. H. (2022): Ultrasonic cavitation: An effective cleaner and greener intensification technology in the extraction and surface modification of nanocellulose. *Ultrasonics Sonochemistry, 90*, 106176.doi: 10.1016/j.ultsonch.2022.106176
37. Li W., Yue J., Liu S. (2012): Preparation of nanocrystalline cellulose via ultrasound and its reinforcement capability for poly (vinyl alcohol) composites. *Ultrasonics Sonochemistry, 19*(3), 479-485. doi: 10.1016/j.ultsonch.2011.11.007
38. Alemdar A., Sain M. (2008): Isolation and characterization of nanofibers from agricultural residues–Wheat straw and soy hulls. *Bioresource technology, 99*(6), 1664-1671. doi: 10.1016/j.biortech.2007.04.029
39. Li R., Fei J., Cai Y., Li Y., Feng J., Yao J. (2009): Cellulose whiskers extracted from mulberry: A novel biomass production. *Carbohydrate Polymers, 76*(1), 94-99. doi: 10.1016/j.carbpol.2008.09.034
40. Chen W., Yu H., Liu Y., Chen P., Zhang M., Hai Y. (2011): Individualization of cellulose nanofibers from wood using high-intensity ultrasonication combined with chemical pretreatments. *Carbohydrate Polymers, 83*(4), 1804-1811. doi: 10.1016/j.carbpol.2010.10.040
41. Madivoli E. S., Kareru P. G., Gachanja A. N., Mugo S. M., Sujee D. M., Fromm K. M. (2022): Isolation of cellulose nanofibers from Oryza sativa residues via TEMPO mediated oxidation. *Journal of Natural Fibers, 19*(4), 1310-1322. doi: 10.1080/15440478.2020.1764454
42. Thygesen A., Oddershede J., Lilholt H., Thomsen A. B., Ståhl K. (2005): On the determination of crystallinity and cellulose content in plant fibres. *Cellulose, 12*, 563-576. doi: 10.1007/s10570-005-9001-8
43. Abraham E., Deepa B., Pothen L. A., Cintil J., et al. (2013): Environmental friendly method for the extraction of coir fibre and isolation of nanofibre. *Carbohydrate Polymers, 92*(2), 1477-1483. doi: 10.1016/j.carbpol.2012.10.056
44. Morán J. I., Alvarez V. A., Cyras V. P., Vázquez A. (2008): Extraction of cellulose and preparation of nanocellulose from sisal fibers. *Cellulose, 15,* 149-159. doi: 10.1007/s10570-007-9145-9
45. Zhang Z., Liu X., Wang H., He H., Bai R. (2021): Preparation and characterization of *Enteromorpha prolifera* nanocellulose/polyvinyl alcohol composite films. *Polymer Composites, 42*(4), 1712-1726. doi: 10.1002/pc.25926
46. Doh H., Lee M. H., Whiteside W. S. (2020): Physicochemical characteristics of cellulose nanocrystals isolated from seaweed biomass. *Food Hydrocolloids, 102*, 105542. doi: 10.1016/j.foodhyd.2019.105542
47. Abd Hamid S. B., Zain S. K., Das R., Centi G. (2016): Synergic effect of tungstophosphoric acid and sonication for rapid synthesis of crystalline nanocellulose. *Carbohydrate polymers, 138*, 349-355. doi: 10.1016/j.carbpol.2015.10.023
48. Saelee K., Yingkamhaeng N., Nimchua T., Sukyai P. (2016): An environmentally friendly xylanase-assisted pretreatment for cellulose nanofibrils isolation from sugarcane bagasse by high-pressure homogenization. *Industrial Crops and Products, 82*, 149-160. doi: 10.1016/j.indcrop.2015.11.064
49. Poy S. Y., Bashir S., Omar F. S., Saidi N. M., et al (2020): Poly (1-vinylpyrrolidone-co-vinyl acetate)(PVP-co-VAc) based gel polymer electrolytes for electric double layer capacitors (EDLC): *Journal of Polymer Research, 27*, 1-10.

doi: 10.1007/s10965-020-2016-x

50. Xiang Z., Gao W., Chen L., Lan W., Zhu J. Y., Runge T. (2016): A comparison of cellulose nanofibrils produced from Cladophora glomerata algae and bleached eucalyptus pulp. *Cellulose, 23*, 493-503. doi: 10.1007/s10570-015-0840-7
51. Jagadeesh D., Jeevan Prasad Reddy D., Varada Rajulu A. (2011): Preparation and properties of biodegradable films from wheat protein isolate. *Journal of Polymers and the Environment, 19*, 248-253. doi: 10.1007/s10924-010-0271-3
52. El Achaby M., Kassab Z., Aboulkas A., Gaillard C., Barakat A. (2018): Reuse of red algae waste for the production of cellulose nanocrystals and its application in polymer nanocomposites. *International Journal of Biological Macromolecules, 106*, 681-691. doi: 10.1016/j.ijbiomac.2017.08.067
53. Zhang Y., Qi J., Zeng W., Huang Y., Yang X. (2020): Properties of dietary fiber from citrus obtained through alkaline hydrogen peroxide treatment and homogenization treatment. *Food Chemistry, 311*, 125873. doi: 10.1016/j.foodchem.2019.125873
54. Valério Filho A., Santana L. R., Motta N. G., Passos L. F., et al. (2023): Extraction of fatty acids and cellulose from the biomass of algae Durvillaea antarctica and Ulva lactuca: An alternative for biorefineries. *Algal Research, 71*, 103084. doi: 10.1016/j.algal.2023.103084
55. Wahlström N., Edlund U., Pavia, H, Toth G., et al. (2020): Cellulose from the green macroalgae Ulva lactuca: isolation, characterization, optotracing, and production of cellulose nanofibrils. *Cellulose, 27*, 3707-3725. doi: 10.1007/s10570-020-03029-5
56. Trubetskaya A., Lê H. Q., Leppiniemi J., Koso T., et al. (2024): Microwave hydrolysis, as a sustainable approach in the processing of seaweed for protein and nanocellulose management. *Algal Research, 78*, 103406. doi: 10.1016/j.algal.2024.103406
57. Haque M. I., Ashraf W., Khan R. I., Shah S. (2022): A comparative investigation on the effects of nanocellulose from bacteria and plant-based sources for cementitious composites. *Cement and Concrete Composites, 125,* 104316. doi: 10.1016/j.cemconcomp.2021.104316
58. Nassiri S., Chen Z., Jian G., ZhongT., et al. (2021): Comparison of unique effects of two contrasting types of cellulose nanomaterials on setting time, rheology, and compressive strength of cement paste. *Cement and Concrete Composites, 123,* 104201. doi: 10.1016/j.cemconcomp.2021.104201